

# An evaluation of air permeability measurements to characterize the saturated hydraulic conductivity of soil reclamation covers

Mingbin Huang<sup>1,2</sup>, Heather Rodger<sup>3</sup>, and S. Lee Barbour<sup>1,4</sup>

<sup>1</sup>Department of Civil and Geological Engineering, University of Saskatchewan, Saskatoon, Saskatchewan, Canada S7N 5A2; <sup>2</sup>The State Key Laboratory of Soil Erosion and Dryland farming on Loess Plateau, ISWC, Northwest A&F University, Yangling, Shaanxi, China; and <sup>3</sup>Norwest Corporation, Vancouver, British Columbia, Canada V6E 3X2. Received 25 July 2014, accepted 17 December 2014. Published on the web 19 December 2014.

Huang, M., Rodger, H. and Barbour, S. L. 2015. **An evaluation of air permeability measurements to characterize the saturated hydraulic conductivity of soil reclamation covers.** *Can. J. Soil Sci.* **95**: 15–26. The saturated hydraulic conductivity ( $K_s$ ) of soil covers used in land reclamation is known to change over time as the result of weathering processes. Guelph permeameter (GP) measurements have been used to track the evolution of  $K_s$  for soil covers at an oil sands mine near Ft. McMurray, Alberta. Although successful, the method was time consuming and consequently a rapid method of estimating  $K_s$  based on in situ air permeability measurements was developed. The objectives of this study were: (1) to use air permeability measurements to characterize the spatial variations of  $K_s$  for typical reclamation soils and (2) to compare air permeability measurements to direct measurements obtained through laboratory and GP measurements. The results highlight that the values of  $K_s$  estimated from measured air permeability values were higher than the values of  $K_s$  measured directly using the GP. This is likely due to swelling of clay soils or air-entrapment during GP measurements. Although the magnitude was over-estimated, the variability of  $K_s$  was captured by the air permeability measurements. Consequently, a limited program of comparative GP and air permeameter measurements could be used to more rapidly characterize the  $K_s$  of reclamation covers over time.

**Key words:** Air permeameter, air permeability, saturated hydraulic conductivity, soil reclamation covers

Huang, M., Rodger, H. et Barbour, S. L. 2015. **Caractérisation de la conductivité hydraulique des sols bonifiés au point de saturation d'après la perméabilité à l'air.** *Can. J. Soil Sci.* **95**: 15–26. On sait que la conductivité hydraulique à saturation ( $K_s$ ) des couvertures de sol évolue avec le temps en raison des phénomènes de météorisation. Les chercheurs ont recouru au perméamètre de Guelph (PG) pour suivre l'évolution de  $K_s$  dans les couches de sol recouvrant un puits d'extraction de sable bitumineux près de Ft. McMurray, en Alberta. Bien qu'efficace, cette méthode s'avère laborieuse, aussi en a-t-on mis au point une plus rapide estimant  $K_s$  à partir de la perméabilité à l'air mesurée in situ. L'étude devait (1) recourir aux relevés de la perméabilité à l'air pour caractériser les variations spatiales de  $K_s$  dans les sols bonifiés et (2) comparer les valeurs de la perméabilité à l'air aux mesures obtenues directement en laboratoire et au moyen du PG. Les résultats indiquent que les valeurs de  $K_s$  estimées à partir de la perméabilité à l'air sont supérieures à celles obtenues directement avec le PG. On le doit sans doute au gonflement des sols argileux ou aux occlusions d'air créées lors de l'utilisation du PG. Malgré cette surestimation, les relevés de la perméabilité à l'air saisissent la variabilité de  $K_s$ . Par conséquent, on pourrait recourir à un programme restreint comparant les relevés du PG et la perméabilité de l'air en vue de caractériser plus rapidement la valeur  $K_s$  des sols bonifiés dans le temps.

**Mots clés:** Perméamètre, perméabilité à l'air, conductivité hydraulique à saturation, couvertures de sol bonifiées

The reclamation covers used at Syncrude's Mildred Lake oil sands mine site are composed of a two-layer cover constructed of a salvaged peat-mineral soil mixture placed over a glacial till soil layer with a cover thickness varying from 35 to 100 cm (Boese 2003). The properties of these reclamation soil covers will evolve over time as a result of changes in secondary structure brought about by processes such as freeze–thaw or wet–dry cycles, settlement of the waste material below the cover, or bioturbation processes caused by rooting or burrowing animals. All of these processes can lead to

the formation of macropores and fractures, which increase the hydraulic conductivity over time (Albrecht and Benson 2001; Meiers et al. 2011).

These changes in hydraulic conductivity can be tracked by repeated measurements of the field saturated hydraulic conductivity ( $K_s$ ) over time. A common method of measuring the  $K_s$  values is through the use of the Guelph permeameter (GP). The GP method consists of a Mariotte type bottle resting on the bottom of a well bore that has been augered into the soil (Elrick and Reynolds 1992). A constant depth of water is maintained

<sup>4</sup>Corresponding author (e-mail: lee.barbour@usask.ca).

**Abbreviations:** AP, air permeameter; GP, Guelph permeameter

in the hole until the water flux from the hole into the soil reaches a constant flow rate ( $Q$ ). The  $K_s$  value can then be estimated from this flow rate based on a number of assumptions related to soil type (Reynolds and Elrick 1986).

Meiers et al. (2011) undertook repeated GP measurements on a reclaimed overburden deposit at the Mildred Lake oil sands mine, operated by Syncrude Canada Ltd., over a 5-yr period. Repeated GP measurements were conducted on an upper soil layer composed of a peat-mineral mixture, an underlying soil cover layer of glacial till, and the underlying shale overburden. The results clearly demonstrated the evolution of the  $K_s$  values of these layers within the first 3 to 4 yr, after which they remained relatively stable.

Although tracking the change in  $K_s$  values in these materials using the GP was successful, it was also time consuming. A single GP measurement (composed of testing with two different water depths) typically requires 10 min to set up and approximately 40 min to conduct the infiltration test in soils with a  $K_s$  value greater than  $1\text{e-}07\text{ m s}^{-1}$ . In soils closer to the limit of the equipment ( $1\text{e-}07$  to  $1\text{e-}09\text{ m s}^{-1}$ ) it may take several hours to conduct a single measurement (Reynolds and Elrick 1986; Meiers et al. 2011).

The air permeability of an unsaturated soil requires a relatively short measurement time as the air flow through the soil reaches steady-state conditions in a matter of seconds. As a consequence, the test has proven useful for the characterization of soil pores and soil structure (Blackwell et al. 1990; Iversen et al. 2003; Wells et al. 2007). The use of air permeability to evaluate saturated hydraulic conductivity is based on the premise that the largest macropores, which have the greatest influence over water flow in saturated soils, are air filled during air permeability testing. In an unsaturated condition, the air permeability of these soils is controlled by the same secondary structure (i.e., larger pores) that controls the  $K_s$ . In a semi-arid region, the water content of the soil during the summer growing season is typically less than field capacity which occurs at matric water potentials of  $-10$  to  $-30\text{ kPa}$  (Iversen et al. 2001). According to capillary theory, pores with diameters greater than  $60$  to  $30\text{ }\mu\text{m}$  will be fully drained at these potentials and consequently are open to air flow. Numerous studies have shown that macroporosity can account for more than 80% of the water flow at or near saturation while it comprises  $<5\%$  of the total porosity of most soils (Watson and Luxmoore 1986; Waduawatte and Si 2004; Kelln et al. 2009). Therefore, the pores contributing to air flow at field capacity are also the dominant pathways for water migration under field saturated conditions.

The ability to undertake rapid testing of air permeability makes it a useful tool to capture spatial, as well as temporal variability in air permeability and by inference,  $K_s$ . The increased use of distributed models requires that the spatial variability of soil physical parameters such as

$K_s$  values be characterized (Poulsen et al. 2001). Loll et al. (1999) used the stochastic analyses of field scale infiltration and ponding during a rainstorm event to evaluate the accuracy and usefulness of the spatial variability of  $K_s$  values as estimated from air permeability. Their results showed that bias appeared between the predicted and measured values, but also revealed that the prediction bias was much less than the sampling uncertainty associated with the estimation of spatial variability in  $K_s$  values from a limited number of samples.

A variety of methods have been used to measure air permeability, including pneumatic tests (Baehr and Hult 1991), dual-probe dynamic pressure technique (Garbesi et al. 1996), and portable air permeameter (Iversen et al. 2001). The portable air permeameter (AP) has several advantages compared with other permeameters. It is easily transported in the field, inexpensive to construct, and simple to repair and operate. Therefore, the portable AP has been used extensively to measure air permeability of shallow agricultural soils, typically to depths of 100 mm (Iversen et al. 2003). In situ measurements of air permeability have also been commonly used in the design of vapour extraction systems used in the remediation of hydrocarbon contaminated sites (Olson et al. 2001; Gogoi et al. 2003).

The objectives of this study were: (1) to evaluate the use of air permeability measurements to characterize spatial variations of  $K_s$  for typical reclamation soils used in the oil sands industry; and (2) to compare air permeability measurements with the results from controlled laboratory tests, as well as field measurements obtained using the Guelph permeameter.

## THEORETICAL BACKGROUND

The movement of a fluid through a porous medium can be described using Darcy's Law as defined below (Freeze 1994):

$$q = \frac{Q}{A} = -K \frac{dh}{dl} \quad (1)$$

where  $q$  is the fluid flux ( $\text{m s}^{-1}$ ),  $Q$  is flow rate ( $\text{m}^3 \text{s}^{-1}$ ),  $A$  is the cross-sectional area across which flow is occurring ( $\text{m}^2$ ),  $h$  is the total head (m), and  $l$  is the length of soil column (m).

The conductivity of a soil to a fluid is a function of both the fluid properties and the intrinsic permeability associated with the geometry of the soil pores as described in the following relationship:

$$K = k\rho g/\mu \quad (2)$$

where  $K$  is the conductivity ( $\text{m s}^{-1}$ ),  $k$  is the intrinsic permeability of the media ( $\text{m}^2$ ),  $\rho$  is the density of the fluid ( $\text{kg m}^{-3}$ ),  $g$  is the gravitational constant ( $\text{m s}^{-2}$ ), and  $\mu$  is the dynamic viscosity of the fluid ( $\text{kg m}^{-1} \text{s}^{-1}$ ) (Freeze and Cherry 1979).

If the intrinsic permeability of the soil was assumed to be the same regardless of whether it was evaluated using water or air, then the intrinsic permeability ( $k$ ), measured using a measurement of air permeability ( $K_a$ ), could be used to calculate  $K_s$  as follows:

$$K_s = \left(\frac{\mu_a}{\rho_a}\right) \left(\frac{\rho_l}{\mu_l}\right) K_a \quad (3)$$

where  $\rho_a$  is the air density ( $\text{kg m}^{-3}$ ),  $\rho_l$  is the water density ( $\text{kg m}^{-3}$ ),  $\mu_a$  is the dynamic viscosity of the air ( $\text{kg m}^{-1} \text{s}^{-1}$ ), and  $\mu_l$  is the dynamic viscosity of the water ( $\text{kg m}^{-1} \text{s}^{-1}$ ).

There are a number of conditions that must be met in order to use Eq. 1 to quantify airflow in a porous media: the flow condition must be laminar, changes in gas volumes due to pressure change must be negligible, and slip flow must not occur.

A non-linear compressible flow equation should theoretically be used instead of Eq. 1 for a compressible fluid. Kirkham (1946) quantified the effects of ignoring compressibility in air flow calculations. He developed a simple AP to measure the intrinsic permeability of soil in the laboratory and field using air pressure differentials which were small relative to atmospheric pressure. The errors associated with neglecting compressibility for applied pressures of approximately 2.5 to 5.0 kPa of air pressure were 1.25 and 2.5%, respectively (Kirkham 1946).

Slip flow occurs because gas velocities are generally non-zero at solid surfaces, resulting in an underestimation of flux according to Darcy's Law (Scanlon et al. 2002). Slip flow is also enhanced in fine-grained material with decreasing air-phase pressure (Ba-Te et al. 2005). Baehr and Hult (1991) found the error associated with ignoring slip flow for in situ air permeability measurements became significant ( $> 10\%$ ) when the values of intrinsic permeability are in the range of  $1 \times 10^{-12} \text{ m}^2$  or less.

## MATERIALS AND METHODS

### Prototype Design

Steinbrenner (1959) proposed one of the original designs of an AP. Later, van Groenewoud (1968), Green and Fordham (1975), and Fish and Koppi (1994) improved on Steinbrenner's design. The AP design used in this study was similar to the AP designs used in agriculture by Iversen et al. (2001). The method of Iversen et al. (2001) was typically used on shallow agricultural soils to a maximum depth of 100 mm. The prototype AP in this study was modified to allow testing to depths of 400 mm.

The AP device consists of a steel cylinder, three flow meters with differing flow ranges, a pressure gauge, a water manometer, a portable nitrogen tank, and a metal cap (Fig. 1). The steel cylinder has a diameter of 160 mm, a wall thickness of 2.0 mm, and a length of 400 mm. The bottom edge of the metal cylinder was sharpened to

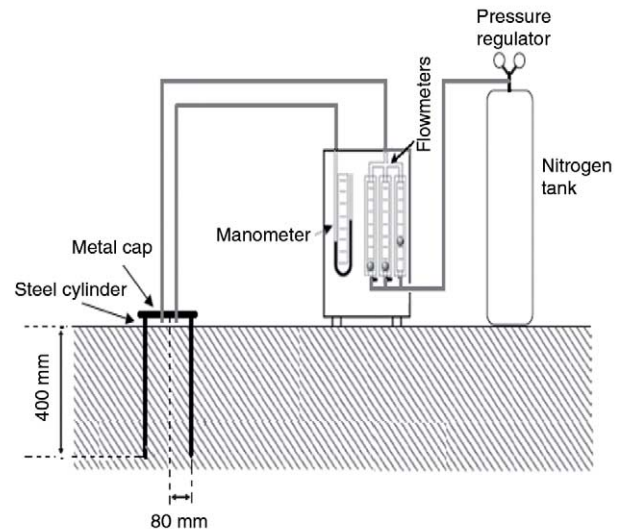


Fig. 1. The schematic and prototype of portable air permeameter.

create a beveled edge such that a small amount of soil is squeezed into the cylinder to help create a seal between the cylinder and the soil. A drop hammer was used in the field to drive the steel cylinder into the soil. A frame was used to support the cylinder during insertion.

A greased rubber gasket was used as a seal between the metal cap and the upper edge of the cylinder during AP measurements. Bolts were used to firmly attach the cap and cylinder through three sets of metal arms welded onto the cap and cylinder. Two threaded ports through the metal cap allowed gas flow into the cylinder during the test and flexible plastic tubing was used to connect the gauges and flow meters to the cylinder.

A portable nitrogen tank (2000 psi capacity) was used as a source of gas for the test. The tank was connected to the flow meters and used to deliver gas at a constant flow rate to the headspace of the steel cylinder. The flow rate used for each test was controlled using one of three flow meters, depending on the required range of flow rates.

The air pressure (gauge) entering the system was set to a value between 0.5 and 1 kPa using the pressure regulator on the outlet of the air tank. Gas supplied to the cylinder passes through the soil contained within the cylinder and is then released by flowing through the soil and back to the atmosphere. The air pressure in the headspace of the steel cylinder was measured using a water manometer.

### Numerical Modeling and Interpretation

Rodger (2007) demonstrated that in a homogeneous soil profile, the majority of the pressure head loss during an AP test occurs across the soil within the steel cylinder. Consequently, in these types of soil profiles, a rapid estimate of air permeability can be obtained by simply substituting the observed gas flux for  $q$  and the observed head spatial change to calculate  $dh/dl$  in Eq. 1. When the soil profile is not homogeneous with depth, the relationship between head loss and flow rate becomes more complicated due to the spatial variability of air permeability and a numerical model is utilized to interpret the field test results.

Wells et al. (2006) demonstrated that an axisymmetric numerical simulation of air flow provided an excellent representation of laboratory gas flow experiments. In this study, an axisymmetric and steady-state flow model (SEEP/W, Geo-Slope 2007) was used to simulate the field measurements and to estimate the air permeability from flow and pressure readings. The model domain was discretized into finite elements with an average element size of 1 cm. A typical model domain is illustrated in Fig. 2. Null elements of zero hydraulic conductivity were used to represent the cylinder wall. Total head (m) boundary conditions representing the measured air pressure were applied to the ground surface inside the cylinder and zero atmospheric pressure was applied to the soil surface outside the cylinder. The lateral and lower boundary conditions were set as zero flux (Fig. 2).

The estimated air permeability is a bulk value for the simulated volume but is dominated by the soil within the cylinder. If the air permeability varied with depth then the value of air permeability for each soil layer would have to be estimated by incorporating the properties of the upper layers in the simulation of the deeper field tests (Rodger 2007).

### Laboratory Evaluation

Controlled laboratory testing was undertaken to verify that the AP method provided estimations of  $K_s$  that were accurate for an inert porous media such as sand. Air permeability and hydraulic conductivity were measured in turn on a column of sand using only air and water,

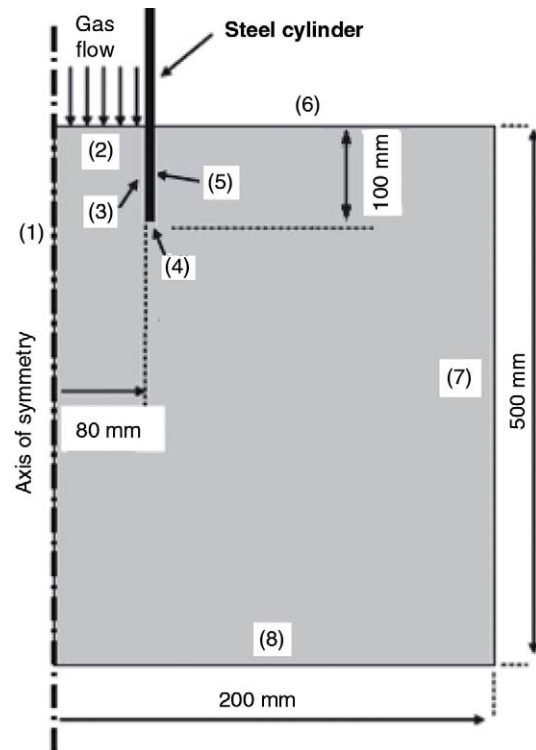


Fig. 2. Simulation domain for an air permeability test in a uniform material. The boundary conditions are: (1) axis of symmetry; (2) delivery pressure; (3) zero flux; (4) zero flux; (5) zero flux; (6) zero pressure; (7) zero flux; and (8) zero flux.

respectively. A large, plastic, rigid wall column, 200 mm in diameter, was filled with dry, uniform sand. The sand was a uniform, natural dune sand locally referred to as Beaver Creek sand and consists of 96.5% sand size particles and 3.6% silt and clay size particles (Bruch 1993).

The head distribution across the column was measured using nine pressure head monitoring ports installed at depths of 40, 55, 70, 110, 150, 190, 230, 245, and 260 mm. Each sampling port was connected to a water manometer. The column test was performed using the same pressure regulator, flow meters and water manometer used for the field AP. Darcy's law was used to calculate the conductivity of the sand for either water or air. Prior to testing  $K_s$  the column was saturated with water, and a hydraulic conductivity test was conducted according to ASTM D2434-68 Standard Test Method for Permeability of Granular Soils (Constant Head) (American Society for Testing and Materials 2005).

A second air permeability test of the same dry sand was also undertaken in a large tank of dry sand using the same AP test setup as was used in the field. The bulk density of dry sand in the tank was the same as the column. The AP was inserted to depths of up to 400 mm in 100-mm increments followed by AP measurements. The boundary effects created by the tank walls were taken into consideration during analysis using the numerical model described previously.

**Field Evaluation**

Field evaluation of the AP was conducted through a program of paired AP and GP measurements undertaken on three different reclamation soil covers on oil sands mine sites. The primary test site was a series of prototype covers constructed over a coke stockpile at the Suncor Energy mine site, referred to as the Suncor Coke site. Coke is a waste by-product from the refinery that has the texture of a medium to coarse sand or gravel. The test cover consisted of a 300 mm surface layer of peat-mineral soil mixture at the surface overlying approximately 350 mm of tailings sand overlying the coke (Fig. 3a).

The second test site was a reclamation cover placed over a shale overburden waste dump located at Syncrude's South Bison Hills at Mildred Lake mine site, referred to as the South Bison Hills site. The reclamation cover constructed at this location had an upper layer of 70 mm of peat-mineral mixture overlying 800 mm layer of glacial till overlying the overburden shale (Fig. 3b).

The third site had a cover constructed over coke at Syncrude Canada's Mildred Lake mine site, referred to as the Coke Beach site. The soil covers were constructed of the same materials as used at South Bison Hills but in this case they were placed over coke rather than overburden shale. The peat-mineral mixture at the test location was 50 mm thick and was underlain by an 800 mm layer of glacial till (Fig. 3c).

The physical properties of the cover soils and tailings sand are shown in Table 1. The peat-mineral mixture had the highest organic matter content, while the tailings sand had the lowest organic matter content.

The AP measurements were conducted at three complete depth profiles of 0 to 400 mm at the South Bison Hills and Coke beach locations and at five complete

depth profiles at the Suncor Coke site. The cylinder was inserted in 100-mm depth increments to a total depth of 400 mm at each test location. A series of 3 to 12 flow rates were applied at each depth increment to establish a relationship between flow and pressure using air pressures ranging from 0.69 to 8.64 kPa.

Guelph permeameter measurements were carried out adjacent to each AP test location at the three sites. A total of three GP measurements were conducted at the South Bison Hills and Coke Beach, respectively, and five GP measurements at the Suncor Coke. The soil sample size of the GP measurements was around 100 cm<sup>3</sup>.

**RESULTS AND DISCUSSION**

**Laboratory Tests**

The flow vs. differential head relationships measured at different depths within the air flow and water flow laboratory columns are shown in Fig. 4a and b, respectively. All measurements demonstrated a linear relationship between flow and head loss. The illustrated hydraulic gradients represent the average response from six separate gas flow rates for air flow measurements and eight different water flow rates for water flow measurements. Figure 4c shows the flow-differential head relationships measured with the AP for different column insertion depths in the laboratory tank test. The linearity of the head loss in proportion to flow rate confirms that the flow regime is laminar over the chosen range of pressures and flow rates. It is important to note that the intercept of the flow vs. differential head relationships were 0 for the water flow column tests but greater than zero for air flow column tests ( $4 \times 10^{-5} \text{ m}^3 \text{ s}^{-1}$  to  $6 \times 10^{-5} \text{ m}^3 \text{ s}^{-1}$ ) and less than zero for the AP tests ( $-3 \times 10^{-5} \text{ m}^3 \text{ s}^{-1}$  to  $-1 \times 10^{-5} \text{ m}^3 \text{ s}^{-1}$ ). Several reasons for this discrepancy were investigated and it was decided that

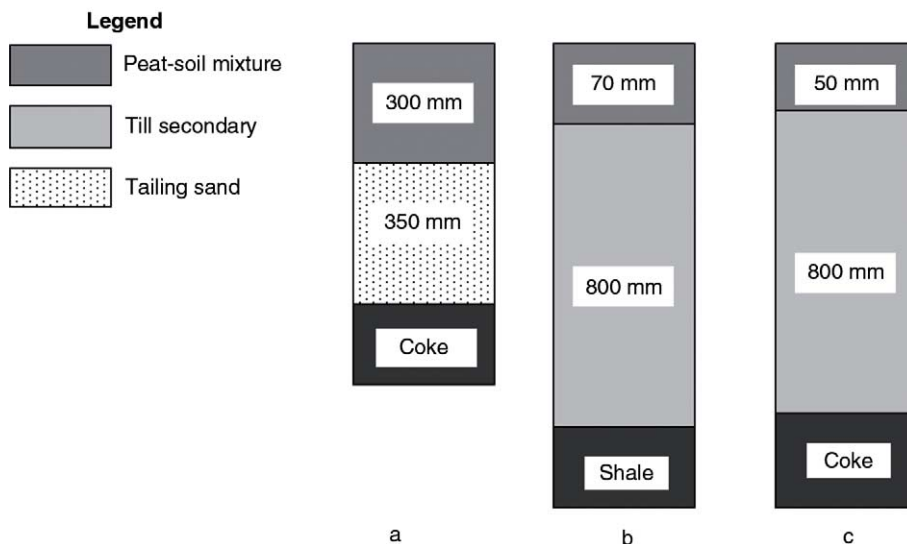


**Fig. 3.** The actual cover prescriptions for field trials at three sites: (a) Suncor Coke, (b) South Bison Hills, and (c) Coke Beach.

**Table 1. Physical properties for peat-soil mixture, tailings sand, peat-mineral mixture, and glacial till material**

Property	Peat-soil mixture	Tailings sand	Peat-mineral mixture	Glacial till
Sand (%)	71.3	93.0	59.5	16.5
Silt (%)	28.6	7.0	29.3	39.0
Clay (%)	0.1	0	11.3	44.5
Porosity	– <sup>z</sup>	–	0.59	0.55
Average bulk density (g cm <sup>-3</sup> )	–	–	0.92 ± 0.31 <sup>y</sup>	1.28 ± 0.21
Organic matter content (%)	–	1.2 <sup>x</sup>	9.3 <sup>w</sup>	4.7 <sup>w</sup>
Soil classification	Loamy sand	Sand	Sandy loam	Silty loam

<sup>z</sup>Not available.<sup>y</sup>Standard deviation.<sup>x</sup>From Khozhina and Sherriff (2006).<sup>w</sup>From McMillan et al. (2007).

slip flow might be the reason for the non-zero intercept for the air-flow tests. The error in ignoring slip effects in permeability calculations was less than 9% according to the result reported by Rodger (2007). A slip correction was applied to selected data using the method described by Scanlon et al. (2002). This adjustment to the data set resulted in a flow-head gradient relationship that did pass through the origin.

The probability distributions of the log transformed  $K_s$  values measured during the two column tests and the prototype field test are presented in Fig. 5. The Shapiro–Wilk test (SAS Institute Inc. 2008) indicated that the  $K_s$  values measured using the air flow column and the AP test were log normally distributed at 0.01 confidence level, while the  $K_s$  values measured using the water flow column were not log normally distributed.

The mean  $K_s$  values measured using the air and water columns were  $7.86 \times 10^{-4} \text{ m s}^{-1}$  and  $7.88 \times 10^{-4} \text{ m s}^{-1}$ , respectively. The difference of less than 1% between these values is insignificant with a  $P$  value of more than 0.8 for the Satterthwaite  $t$  test (SAS Institute Inc. 2008). This confirms that for a non-reactive porous media, the intrinsic permeability measured using either air or water as the fluid is identical when measured under controlled laboratory conditions. The mean value of  $K_s$  determined using the prototype field AP was  $9.01 \times 10^{-4} \text{ m s}^{-1}$ . This value has a relative difference of 14% from the water column measurement. Although the difference is significant ( $P < 0.01$ ), this error is acceptable for the purpose of field AP measurements. Reynolds and Elrick (1987) found that the GP measurements often resulted in an underestimate of the actual  $K_s$  from 17% to a third order of magnitude due to the entrapped air. The laboratory AP measurements had a very small variability among the repeated tests with a standard deviation (STD) value of  $0.79 \times 10^{-4} \text{ m s}^{-1}$ , less than a STD value of  $1.20 \times 10^{-4} \text{ m s}^{-1}$  for the water flow column measurement and a STD value of  $1.21 \times 10^{-4} \text{ m s}^{-1}$  for the air flow column measurement.

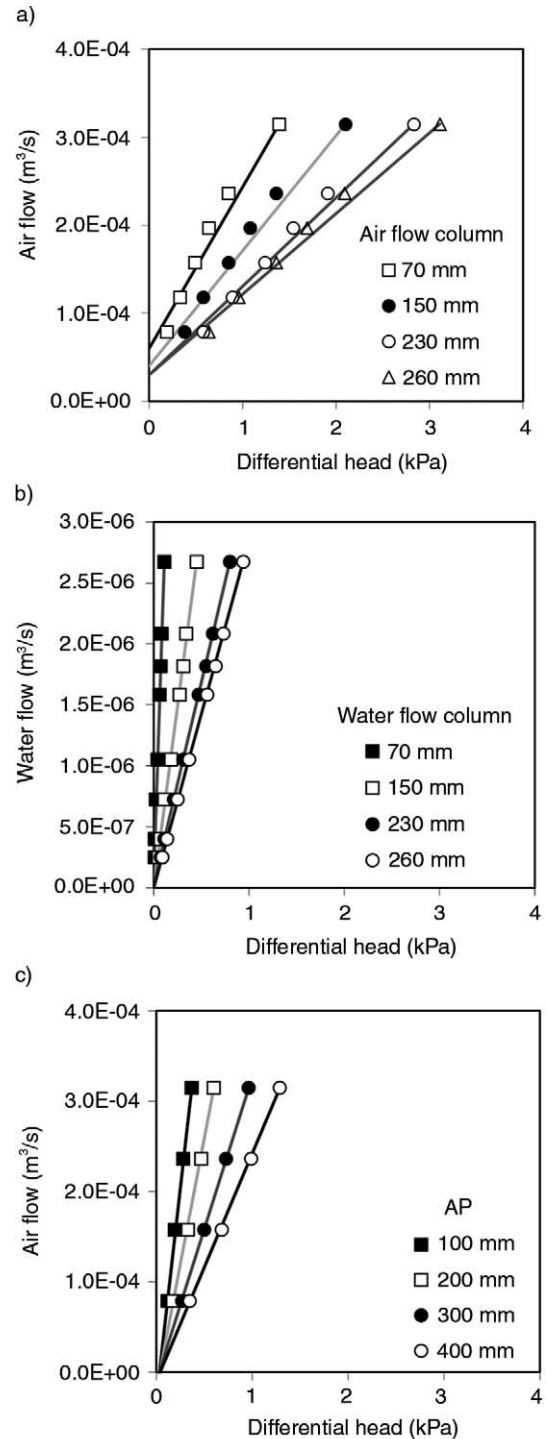


**Fig. 4.** The flow-differential head curves observed at differing depths for (a) the air flow column, (b) the water flow column, and (c) air flow tank tests.

The good agreement between the various methods of measuring  $K_s$  values highlighted the ability of the AP technique to provide a reliable measurement of  $K_s$  under controlled conditions.

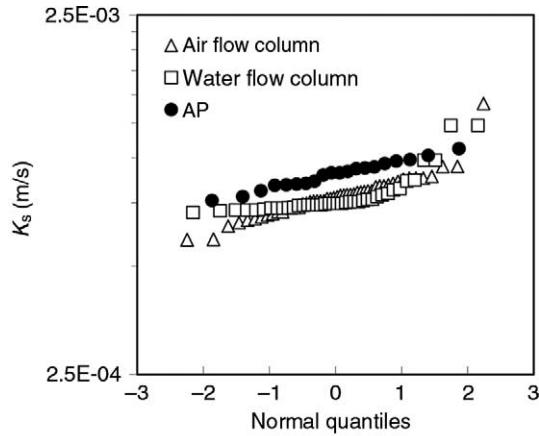


Fig. 5. Probability distributions of the saturated hydraulic conductivity ( $K_s$ ) measurements using a column with air as the test fluid, a column with water as the test fluid, and the AP in a sand tank.

### Field Measurements of Saturated Hydraulic Conductivity Using the AP

Figure 6a–c shows a typical set of flow-pressure data for each depth at the three study sites. The majority of the flow-pressure data sets from the field demonstrated a linear relationship between flow rate and pressure with an intercept of zero. Several of the flow-pressure data sets did have a non-zero intercept varying from  $4 \times 10^{-6} \text{ m}^{-3} \text{ s}^{-1}$  to  $2 \times 10^{-5} \text{ m}^{-3} \text{ s}^{-1}$  similar to the laboratory air flow tests (Fig. 4a and c). The effect of slip flow was still considered as a main reason. Weeks (1978) and Wells et al. (2007) demonstrated that slip flow may be significant for soils with high silt and clay fractions.

The mean and STD of  $K_s$  values estimated for the three sites are summarized according to the location and depth of cylinder insertion in Table 2. The frequency distributions at the different depths are shown in Figs. 7a–c.

At the Suncor Coke site, the mean values of  $K_s$  varied from  $2.65 \times 10^{-5}$  to  $6.53 \times 10^{-5} \text{ m s}^{-1}$  and the  $K_s$  values suggested there was significantly spatial variability between the five locations according to the ANOVA analysis (SAS Institute Inc. 2008). The measured  $K_s$  values using the AP within the top 0–100 mm layer show the greatest variability, with a STD of  $4.07 \times 10^{-5} \text{ m}^{-1} \text{ s}^{-1}$  (Table 2), while the remaining layers had STD values in the range of  $0.93 \times 10^{-5}$  to  $1.15 \times 10^{-5} \text{ m s}^{-1}$ . The higher variability in the top layer may be due to the fact that the peat–mineral mixture is not a well-controlled mixture since it is derived simply from overstripping of organic rich material with the underlying mineral soil. The mean values of  $K_s$  estimated using the AP at the four depths were  $4.90 \times 10^{-5} \text{ m s}^{-1}$ ,  $2.82 \times 10^{-5} \text{ m s}^{-1}$ ,  $5.21 \times 10^{-5} \text{ m s}^{-1}$ , and  $4.11 \times 10^{-5} \text{ m s}^{-1}$ , respectively with increasing depth.

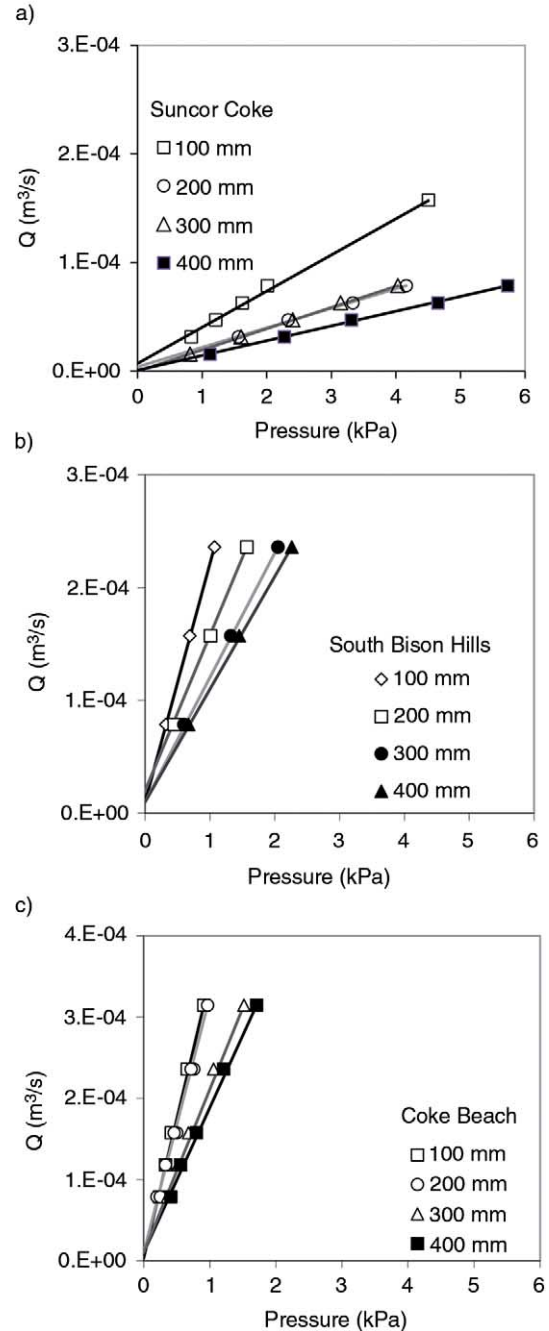


Fig. 6. Pressure flow curves observed at differing depths for field AP measurements at three sites.

At the South Bison Hills, the mean values of  $K_s$  varied from  $2.05 \times 10^{-4}$  to  $6.11 \times 10^{-4} \text{ m s}^{-1}$  at three locations. The  $K_s$  values at the first location were significantly smaller than those at the second and third locations, while no significant difference in  $K_s$  values was found between the second and third locations. At different depths, the measured  $K_s$  values were all quite similar, both in order of magnitude and variability, although the 200- to 300-mm

**Table 2.** The mean and standard deviation of saturated hydraulic conductivity ( $K_s$ ) values measured using an air permeameter (AP) at different locations and depths for all sites and their significance tests

Treatment	Suncor Coke			South Bison Hills			Coke Beach		
	<i>n</i>	Mean ( $\text{m s}^{-1}$ )	STD <sup>2</sup>	<i>n</i>	Mean ( $\text{m s}^{-1}$ )	STD	<i>n</i>	Mean ( $\text{m s}^{-1}$ )	STD
Location									
1	19	$4.66 \times 10^{-5}a$	$0.68 \times 10^{-5}$	18	$2.05 \times 10^{-4}a$	$0.51 \times 10^{-4}$	26	$6.01 \times 10^{-4}a$	$1.78 \times 10^{-4}$
2	21	$6.53 \times 10^{-5}a$	$3.81 \times 10^{-5}$	26	$4.00 \times 10^{-4}b$	$0.97 \times 10^{-4}$	23	$9.71 \times 10^{-4}b$	$6.79 \times 10^{-4}$
3	19	$2.65 \times 10^{-5}b$	$0.98 \times 10^{-5}$	12	$6.11 \times 10^{-4}b$	$2.99 \times 10^{-4}$	27	$6.41 \times 10^{-4}c$	$1.55 \times 10^{-4}$
4	31	$3.55 \times 10^{-5}bc$	$1.56 \times 10^{-5}$	–	–	–	–	–	–
5	18	$4.86 \times 10^{-5}ac$	$2.20 \times 10^{-5}$	–	–	–	–	–	–
Depth									
0–100 mm	30	$4.90 \times 10^{-5}ABC$	$4.07 \times 10^{-5}$	12	$2.49 \times 10^{-4}A$	$0.92 \times 10^{-4}$	13	$5.64 \times 10^{-4}A$	$3.30 \times 10^{-4}$
100–200 mm	20	$2.82 \times 10^{-5}A$	$1.10 \times 10^{-5}$	18	$4.27 \times 10^{-4}B$	$2.16 \times 10^{-4}$	24	$6.04 \times 10^{-4}A$	$3.36 \times 10^{-4}$
200–300 mm	29	$5.21 \times 10^{-5}B$	$1.15 \times 10^{-5}$	9	$5.21 \times 10^{-4}AB$	$3.32 \times 10^{-4}$	19	$9.71 \times 10^{-4}A$	$5.88 \times 10^{-4}$
300–400 mm	29	$4.11 \times 10^{-5}C$	$0.93 \times 10^{-5}$	17	$3.55 \times 10^{-4}AB$	$1.25 \times 10^{-4}$	14	$9.77 \times 10^{-4}A$	$6.62 \times 10^{-4}$
Total	108	$4.39 \times 10^{-5}$	$2.45 \times 10^{-5}$	56	$3.88 \times 10^{-4}$	$1.15 \times 10^{-4}$	70	$7.77 \times 10^{-4}$	$2.28 \times 10^{-4}$

<sup>2</sup>Standard deviation.

*a-c*, *A-C* Treatments are significantly different at  $P=0.01$  confidence level with different letters.

layer had slightly more variability than the other three layers (Fig. 7b and Table 2). The mean values of  $K_s$  at the four depths were  $2.49 \times 10^{-4} \text{ m s}^{-1}$ ,  $4.27 \times 10^{-4} \text{ m s}^{-1}$ ,  $5.21 \times 10^{-4} \text{ m s}^{-1}$ , and  $3.55 \times 10^{-4} \text{ m s}^{-1}$ , in order of increasing depth. The mean value in the first depth reflects the hydraulic conductivity of a 70-mm-thick peat-mineral mixture and 30-mm-thick glacial till layer, while the other values were representative of the glacial till layers alone. The difference of  $K_s$  values at the three depths (100–200 mm, 200–300 mm, and 300–400 mm) was not significant. The  $K_s$  values determined on this cover were more uniform than those determined at the Suncor Coke covers. This is likely due to the uniform nature of the weathered glacial till soils at South Bison Hills.

The mean values of  $K_s$  at the three Coke Beach locations were  $6.01 \times 10^{-4} \text{ m s}^{-1}$ ,  $9.71 \times 10^{-4} \text{ m s}^{-1}$ , and  $6.41 \times 10^{-4} \text{ m s}^{-1}$ , respectively, and the values of  $K_s$  were considered to be significantly different between two of them. For the four depths, the mean values of  $K_s$  varied from  $5.64 \times 10^{-4}$  to  $9.77 \times 10^{-4} \text{ m s}^{-1}$ . Except for the first depth increment, these  $K_s$  values are primarily for the glacial till layer, since the peat-mineral layer was only 50 mm thick at this location.

These mean values are all within 28.4% of each other and their difference was not significant at 0.01 confidence level. The glacial till cover soil at both of the Syncrude sites are similar in texture and are both weathered as the result of freeze–thaw and wet–dry cycles, although the cover soils at the Suncor Coke site are generally drier than those at the South Bison Hills.

Among the three sites, the mean value of  $K_s$  at the Suncor Coke site ( $4.39 \times 10^{-5} \text{ m s}^{-1}$ ) was approximately one order of magnitude smaller than that at the South Bison Hills ( $3.88 \times 10^{-4} \text{ m s}^{-1}$ ) and Coke Beach ( $7.77 \times 10^{-4} \text{ m s}^{-1}$ ) sites (Table 2). The fact that the Syncrude sites' soils have a higher  $K_s$  value than the sand is not surprising since these glacial till soils are clay-rich (Table 1) and are

heavily weathered from repeated wet–dry and freeze–thaw cycles. The presence of secondary structures such as cracks can significantly increase the  $K_s$  value. Kelln et al. (2009) found the macropores and secondary structure within the cover soils at the South Bison Hills site occupied 3–4% of the total soil volume with an average pore size from  $1 \times 10^{-5}$  to  $1 \times 10^{-3} \text{ m}$ .

### Comparison of the AP and GP Tests

Guelph permeameter measurements were also carried out adjacent to each AP test profile and the measured hydraulic conductivity using the GP was assumed to represent the average value in the profile from 0 to 400 mm. The probability distributions of the hydraulic conductivity measured with the GP and estimated from AP for all materials involved in this study are shown in Fig. 8a–c. For each soil cover, the AP results are for the whole profile (0 to 400 mm) in all trials.

A number of researchers have used the GP test to measure the hydraulic conductivity of the cover soils at the Suncor Coke and the two Syncrude covers. Due to the limited number of GP measurements, Fig. 8a–c also included additional GP measurements at the same sites obtained by other researchers (Fenske 2007; O'Kane 2007; Kelln et al. 2008; Meiers et al. 2011). The average value from these  $K_s$  measurements was  $1.06 \times 10^{-6} \text{ m s}^{-1}$  for the peat–soil mixture at the Suncor Coke site (nine measurements),  $3.13 \times 10^{-6} \text{ m s}^{-1}$  for the glacial till at South Bison Hills (12 measurements), and  $0.53 \times 10^{-6} \text{ m s}^{-1}$  for the glacial till at Coke Beach (14 measurements). All of these  $K_s$  measurements were conducted after the hydraulic conductivity evolution as a result of freeze–thaw and wet–dry weathering was assumed to be complete. The values of  $K_s$  are consistent with the mean value obtained for each cover using the GP in this study.

The AP tests overestimated the values of  $K_s$  for the materials at the three sites in comparison with that obtained using the GP. There is approximately one



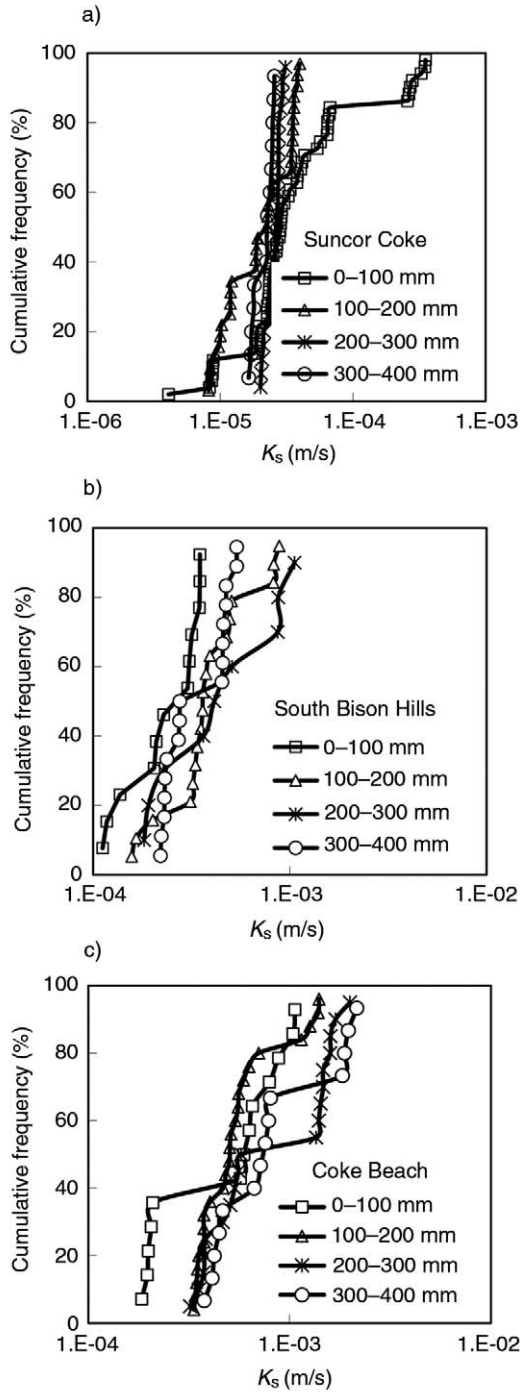


**Fig. 7.** Probability distributions of the saturated hydraulic conductivity measurements ( $K_s$ ) at (a) Suncor Coke, (b) South Bison Hills, and (c) Coke Beach for four depth trials.

order of magnitude difference in the median values of  $K_s$  measured with the AP and GP methods for the upper layer at the Suncor Coke site (Fig. 8a). The median value for the AP tests in this study was  $2.89 \times 10^{-5} \text{ m s}^{-1}$ , while the median value for the GP tests was  $1.49 \times 10^{-6} \text{ m s}^{-1}$ .

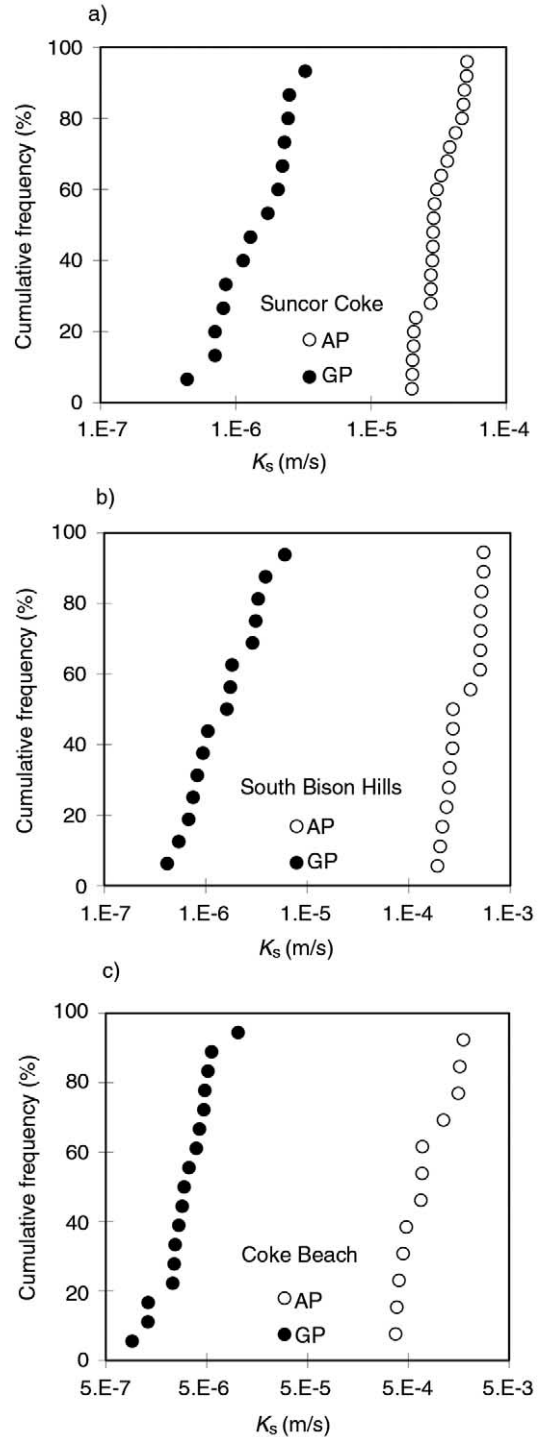


**Fig. 8.** Probability distributions of the field-measured saturated hydraulic conductivity ( $K_s$ ) using the air (AP) and Guelph (GP) permeameters at three sites.

The median values of  $K_s$  for the two Syncrude covers measured using the AP and the GP are consistently two orders of magnitude different (Fig. 8b and c). The median values of  $K_s$  on the South Bison Hills cover was

$2.72 \times 10^{-4} \text{ m s}^{-1}$  for the AP tests and  $1.62 \times 10^{-6} \text{ m s}^{-1}$  for the GP tests, while the AP median values on the Coke Beach cover was  $6.74 \times 10^{-4} \text{ m s}^{-1}$  and the median values for the GP tests was  $2.97 \times 10^{-6} \text{ m s}^{-1}$ .

There are many possible reasons for the observed differences between the AP and GP tests in this study. One explanation may be that the GP underestimated the  $K_s$  value for the studied materials. The materials in these covers are predominantly fine-grained with an extensive macropore network as a result of weathering and bioturbation processes (Meiers et al. 2011). During a GP measurement, the swelling and changes of the macropore structure that occur in clay-rich soil covers when exposed to freshwater will lead to a reduction in the available area for flow and an underestimation of field  $K_s$  (Blackwell et al. 1990).

The effect of air entrapment during infiltration can also lead to an underestimation of  $K_s$  by about a half order of magnitude when using the GP (Reynolds and Elrick 1986). The impact of air entrapment can be particularly significant for clay soils where the magnitude of  $K_s$  is governed by macropores. Reynolds and Zebchuk (1996) have evaluated the use of the GP method to measure  $K_s$  in a clay soil, and found that the GP accuracy in medium- and fine-textured soil was not well established and the measured  $K_s$  values were highly variable with a range of about three orders of magnitude.

Another explanation for the differences of the AP and GP tests at the three sites may be due to the high degree of anisotropy in the reclamation soils. The macropore network formed as a result of desiccation or freeze-thaw, as well as bioturbation processes, are likely to create higher hydraulic conductivity in the top 0.5 m of the soil. Chief et al. (2008) examined the potential impacts of anisotropy on in situ intrinsic permeability measurements, and found that anisotropic conditions might introduce a significant error (two orders of magnitude) in intrinsic permeability estimates. In this study, the ratios of the cylinder diameter (D) to the inserted depths (H) varied from 0.4 to 1.6. As a result, based on the results of Chief et al. (2008), the measured air permeability would not be sensitive to horizontal  $K_s$  values. The AP measures flow in the vertical direction and captures the maximum vertical conductivity of the soil. The GP response is dominated initially by lateral flow in response to existing negative pore pressures within the soil (Reynolds and Elrick 1986); however, this transitions to more vertical flow as the flow rate stabilizes. Regardless, the GP results will be more affected by horizontal  $K_s$  than that of the AP.

In addition, the GP may have underestimated  $K_s$  values due to the small volume of soil tested. Mohanty et al. (1994) found that small sample size resulted in the GP underestimating  $K_s$  values. In this study, the measured sample size was around  $100 \text{ cm}^3$  for the GP method and  $2010 \text{ cm}^3$  for the AP method.

Although the AP test overestimated the  $K_s$  value for each site, similar probability distributions for the  $K_s$  values from the AP and GP tests were obtained at each site. In order to verify the similarity of probability distributions for the  $K_s$  values from AP and GP tests at each site, all the measured values shown in Fig. 8a–c were normalized by dividing the log values by the log transformed median value. The new cumulative probability distributions are shown in Table 3. A paired  $t$  test was used to assess the difference in probability distributions for the AP and GP tests at each site (SAS Institute Inc. 2008) and the results are shown in Table 3. The paired  $t$  tests show that at the three sites, the normalized probability distributions for the  $K_s$  values from AP and GP tests were not significantly different at the 0.01 confidence level.

Other researchers have noted a similar correlation in the probability distributions of  $K_s$  values estimated using AP methods and measured directly in the laboratory or field. Empirical relationships between air permeability and the measured  $K_s$  at  $-10 \text{ kPa}$  have been proposed in the literature (Iversen et al. 2003). Loll et al. (1999) developed a general predictive relationship between air permeability and  $K_s$  based on the results from two studies (Schjonning 1986; Riley and Ekeberg 1989), which involved air permeability and  $K_s$  laboratory measurements on 1614 undisturbed soil cores. Both Schjonning (1986) and Riley and Ekeberg (1989) found a log–log linear relationship to exist between the laboratory measurements of air permeability and  $K_s$ . Iversen et al. (2004) tested the suitability of the relationship developed by Loll et al. (1999) for predicting  $K_s$  from in situ air permeability measurements using the portable AP. The parallel measurements of air permeability and  $K_s$  showed a good agreement between the predicted and measured  $K_s$  values with an error of  $\pm 0.7$  orders of magnitude. Unfortunately, these approaches were unable to be evaluated in this study due to the limited number of GP measurements.

**Table 3. The results of the paired  $t$  test for the similarity of probability distribution between air permeameter (AP) and Guelph permeameter (GP) tests. The values shown in the table are normalized by dividing the log values by the log transformed median values**

Cumulative probability (%)	Suncor Coke		South Bison Hills		Coke Beach	
	AP	GP	AP	GP	AP	GP
99	0.945	0.941	0.916	0.902	0.869	0.903
95	0.946	0.941	0.916	0.902	0.869	0.903
90	0.947	0.962	0.916	0.934	0.880	0.950
75	0.969	0.968	0.924	0.951	0.908	0.964
50	1.0	1.0	1.0	1.0	1.0	1.0
25	1.021	1.045	1.012	1.058	1.064	1.018
10	1.034	1.056	1.035	1.082	1.077	1.065
5	1.034	1.091	1.043	1.102	1.081	1.093
1	1.035	1.091	1.043	1.102	1.081	1.093
$t$ value	2.28		2.59		1.51	
$P$ value	0.052		0.032		0.169	

## CONCLUSIONS

Tracking the changes in hydraulic conductivity is an important step in assessing the long-term performance of a reclamation soil cover. However, tracking hydraulic conductivity over large cover areas and over multiple years using in situ testing of water hydraulic conductivity is prohibitive. Since it requires only a short measuring time, the AP method is a potential alternative to traditional methods of field  $K_s$  measurement. However, further investigation is required before this method can be determined to be reliable.

Several factors were discussed throughout this paper which may contribute to the difference in hydraulic conductivity. Some of these factors include macropore flow, air entrapment, smearing of fine-grained materials, and slip flow. Understanding of these factors could possibly be gained by comparing the AP with other methods of  $K_s$  measurement.

The AP was found to provide an acceptable value of hydraulic conductivity under ideal, controlled, laboratory conditions with dry sand. However, in the case of fine-textured, heterogeneous, and potentially anisotropic field soils, the differences in measured values of hydraulic conductivity using the AP and GP were substantial. Still, it is important to note that the variation in hydraulic conductivity captured by each method was similar, with probability distributions which showed no significant difference at a 0.01 level of confidence. This suggests that a limited program of parallel testing using both GP and AP testing could be used to establish a reliable correlation to estimate the field saturated hydraulic conductivity from AP test results. The AP test method could then be used to characterize variability (spatial and temporal).

## ACKNOWLEDGEMENTS

The authors would like to acknowledge the financial support of Syncrude Canada Ltd., and Suncor Energy, as well as the National Sciences and Engineering Research program (NSERC).

**Albrecht, B. A. and Benson, C. H. 2001.** Effect of desiccation on compacted natural clays. *J. Geotech. Geoenviron. Eng.* **127**: 67–75.

**American Society for Testing and Materials. 2005.** D2434-68 Standard test method for permeability of granular soils (Constant head), Annual Book of ASTM Standards 2005, Volume 04.08, ASTM International, West Conshohocken, PA.

**Baehr, A. L. and Hult, M. F. 1991.** Evaluation of unsaturated zone air permeability through pneumatic tests. *Water Resour. Res.* **27**: 2605–2617.

**Ba-Te, Zhang, L. and Fredlund, D. G. 2005.** A general air phase permeability function for airflow through unsaturated soils, *Geo-Frontiers 2005 Congress*. P. E. Ellen and M. Rathje, eds. 2005 Jan. 24–26, 2005. American Society of Civil Engineering, Austin, TX.

**Blackwell, P. S., Ringrose-Voase, A. J., Jayawardane, N. S., Olsson, K. A., McKenzie, D. C. and Mason, W. K. 1990.** The use of air-filled porosity and intrinsic permeability to air to

characterize structure of macropore space and saturated hydraulic conductivity of clay soils. *J. Soil Sci.* **41**: 215–228.

**Boese, C. D. 2003.** The design and installation of a field instrumentation program for the evaluation of soil atmosphere water fluxes in a vegetated cover over saline/sodic shale overburden. M.Sc. thesis. Department of Civil and Geological Engineering, University of Saskatchewan, Saskatoon, SK.

**Bruch, P. G. 1993.** A laboratory study of evaporative fluxes in homogeneous and layered soils. M.Sc. thesis, University of Saskatchewan, Saskatoon, SK.

**Chief, K., Ferré, T. P. A. and Hinnell, A. C. 2008.** The effects of anisotropy on In situ air permeability measurements. *Vadose Zone J.* **7**: 941–947.

**Elrick, D. E. and Reynolds, W. D. 1992.** Infiltration from constant-head well permeameters and infiltrometers. *Advances in measurement of soil physical properties: Bringing theory into practice*, Special Publ. no. 30. SSSA, Madison, WI. pp. 1–24.

**Fenske, D. 2007.** A study to evaluate the performance of a reclamation soil cover placed over an oil sands fluid coke deposit. M.Sc. thesis. Department of Civil and Geological Engineering, University of Saskatchewan, Saskatoon, SK.

**Fish, A. N. and Koppi, A. J. 1994.** The use of a simple field air permeameter as a rapid indicator of functional soil pore space. *Geoderma* **63**: 255–264.

**Freeze, R. A. 1994.** Henry Darcy and the fountains of Dijon. *Ground Water* **32**: 23–30.

**Freeze, R. A. and Cherry, J. A. 1979.** *Groundwater*. Prentice-Hall, Inc., Englewood Cliffs, NJ.

**Garbesi, K., Sextro, R. G., Robinson, A. L., Wooley, J. D. and Owens, J. A. 1996.** Scale dependence of soil permeability to air: Measurement method and field investigation. *Water Resour. Res.* **32**: 547–560.

**Geo-Slope International, Ltd. 2007.** *GeoStudio 2007*. Calgary, AB.

**Gogoi, B., Dutta, N., Goswami, P. and Mohan, T. 2003.** A case study of bioremediation of petroleum-hydrocarbon contaminated soil at a crude oil spill site. *Adv. Environ. Res.* **7**: 767–782.

**Green, R. D. and Fordham, S. J. 1975.** A field method for determining air permeability in soil. *Soil physical conditions and crop production*. Tech. Bull. 29. Soil Survey of England and Wales.

**Iversen, B. V., Moldrup, P. and Loll, P. 2004.** Runoff modeling at two field slopes: Use of in situ measurements of air permeability to characterize spatial variability of saturated hydraulic conductivity. *Hydrol. Proc.* **18**: 1009–1026.

**Iversen, B. V., Moldrup, P., Schjonning, P. and Jacobsen, O. H. 2003.** Field application of a portable air permeameter to characterize spatial variability in air and water permeability. *Vadose Zone J.* **2**: 618–626.

**Iversen, B. V., Schjonning, P., Poulsen, T. G. and Moldrup, P. 2001.** In situ, on-site and laboratory measurements of soil air permeability: Boundary conditions and measurement scale. *Soil Sci.* **166**: 97–106.

**Kelln, C., Barbour, S. L. and Qualizza, C. V. 2009.** Fracture-dominated subsurface flow and transport in a sloping reclamation cover. *Vadose Zone J.* **8**: 96–107.

**Kelln, C., Barbour, S. L. and Qualizza, C. 2008.** Controls on the spatial distribution of soil moisture and solute transport in a sloping reclamation cover. *Can. Geotech. J.* **45**: 351–366.

**Khodzina, E. I. and Sherriff, B. 2006.** Background research of the tailings area of a Ni-Cu mine for the determination of an

optimal method of revegetation. *For. Snow Landsc. Res.* **80**: 367–386.

**Kirkham, D. 1946.** Field method for determination of air permeability of soil in its undisturbed state. *SSSA Proc.* **11**: 93–99.

**Loll, P., Moldrup, P., Schjonning, P. and Riley, H. 1999.** Predicting saturated hydraulic conductivity from air permeability: Application in stochastic water infiltration modeling. *Water Resour. Res.* **35**: 2387–2400.

**McMillan, R., Quideau, S. A., MacKenzie, M. D. and Biryukova, O. 2007.** Nitrogen mineralization and microbial activity in oil sands reclaimed boreal forest soils. *J. Environ. Qual.* **36**: 1470–1478.

**Meiers, G., Barbour, S. L., Qualizza, C. and Dobchuk, B. 2011.** Evolution of the hydraulic conductivity of reclamation covers over sodic/saline mining overburden. *J. Geotech. Geoenviron. Eng.* **137**: 968–976.

**Mohanty, B. P., Kanwar, R. S. and Everts, C. J. 1994.** Comparison of saturated hydraulic conductivity measurement methods for a glacial-till soil. *SSSA J.* **58**: 672–677.

**O'Kane Consultants Inc. 2007.** As-built report for the coke stockpile automated meteorological station and In situ soil monitoring stations at Suncor Energy Inc. O'KC Report No. 706/05–02. Saskatoon, SK.

**Olson, M. S., Tillman, F. D. J., Choi, J. W. and Smith, J. A. 2001.** Comparison of three techniques to measure unsaturated-zone air permeability at Picatinny Arsenal, NJ. *J. Contam. Hydrol.* **53**: 1–19.

**Poulsen, T. G., Iversen, B. V., Yamaguchi, T., Moldrup, P. and Schjonning, P. 2001.** Spatial and temporal dynamics of air permeability in a constructed field. *Soil Sci.* **166**: 153–162.

**Reynolds, W. D. and Elrick, D. E. 1986.** A method for simultaneous in situ measurement in the vadose zone of field-saturated hydraulic conductivity, sorptivity and the conductivity-pressure head relationship. *Ground Water Monit. Rev.* **6**: 84–95.

**Reynolds, W. D. and Elrick, D. E. 1987.** A laboratory and numerical assessment of the Guelp permeameter method. *Soil Sci.* **144**: 282–292.

**Reynolds, W. D. and Zebchuk, W. D. 1996.** Hydraulic conductivity in a clay soil: Two measurement techniques and spatial characterization. *Soil Sci. Soc. Am. J.* **60**: 1679–1685.

**Riley, H. and Ekeberg, E. 1989.** Ploughless tillage in large-scale trials, II, Studies of soil chemical and physical properties. *Norsk Landbrugsforsk.* **3**: 107–115.

**Rodger, H. A. 2007.** Tracking changes in hydraulic conductivity of soil reclamation covers with the use of air permeability measurements. M.Sc. thesis. Department of Civil and Geological Engineering, University of Saskatchewan, Saskatoon, SK.

**SAS Institute Inc. 2008.** SAS/STAT users' guide, Release 9.2 ed. SAS Institute Inc., Cary, NC.

**Scanlon, B. R., Nicot, J. P. and Massmann, J. W. 2002.** Chapter 8. Soil gas movement in unsaturated systems. *Soil Physics Comp.* pp. 297–341.

**Schjonning, P. 1986.** Soil permeability by air and water as influenced by soil type and incorporation of straw. *Tidsskrift for Planteavl* **90**: 227–240.

**Steinbrenner, E. C. 1959.** A portable air permeameter for forest soils. *Soil Sci. Soc. Am. Proc.* **23**: 478–481.

**van Groenewoud, H. 1968.** Methods and apparatus for measuring air permeability of the soil. *Soil Sci.* **106**: 275–279.

**Waduawatte, B. and Si, B. C. 2004.** Near-saturated surface soil hydraulic properties under different land uses in the St. Denis National Wildlife Area, Saskatchewan, Canada. *Hydrol. Processes* **18**: 2835–2850.

**Watson, K. W. and Luxmoore, R. J. 1986.** Estimating macroporosity in a forest watershed by use of a tension infiltrometer. *Soil Sci. Soc. Am. J.* **50**: 578–582.

**Weeks, E. P. 1978.** Field determination of vertical permeability to air in the unsaturated zone. USGS Pap. 1051. US Gov. Print. Office, Washington, DC.

**Wells, T., Fityus, S. and Smith, D. W. 2007.** Use of in situ air flow measurements to study permeability in cracked clay soils. *J. Geotech. Geoenviron. Eng.* **133**: 1577–1586.

**Wells, T., Fityus, S., Smith, D. W. and Moe, H. 2006.** The indirect estimation of saturated hydraulic conductivity of soils, using measurements of gas permeability. I. Laboratory testing with dry granular soils. *Aust. J. Soil Res.* **44**: 719–725.